Journal of Alloys and Compounds 642 (2015) 232–237

Contents lists available at ScienceDirect

Journal of Alloys and Compounds

journal homepage: www.elsevier.com/locate/jalcom

Disorder- and correlation-induced charge carriers localization in oxyborate $MgFeBO_4$, $Mg_{0.5}Co_{0.5}FeBO_4$, $CoFeBO_4$ single crystals

Yu.V. Knyazev [a], N.V. Kazak [b,*], M.S. Platunov [b], N.B. Ivanova [a], L.N. Bezmaternykh [b], A. Arauzo [c], J. Bartolomé [d], S.G. Ovchinnikov [a,b,e]

[a] Siberian Federal University, 660074 Krasnoyarsk, Russia
[b] Kirensky Institute of Physics, 660036 Krasnoyarsk, Russia
[c] Servicio de Medidas Físicas, Universidad de Zaragoza, 50009 Zaragoza, Spain
[d] Instituto de Ciencia de Materiales de Aragón, CSIC-Universidad de Zaragoza and Departamento de Física de la Materia Condensada, 50009 Zaragoza, Spain
[e] Siberian State Aerospace University, 660014 Krasnoyarsk, Russia

ARTICLE INFO

Article history:
Received 14 December 2014
Received in revised form 18 March 2015
Accepted 7 April 2015
Available online 18 April 2015

Keywords:
Transition metal alloys and compounds
Disordered system
Semiconductors
Electrical transport

ABSTRACT

The temperature dependence of the resistivity of single crystalline $Mg_{1-x}Co_xFeBO_4$ samples with $x = 0.0$, 0.5, 1.0 is investigated for the temperature range (210–400 K). The conduction was found to be governed by Mott variable-range hopping (VRH) in the low-temperature range ($T = 210$–270 K) and by thermo-activation mechanism in the high-temperature range ($T = 280$–400 K). Microscopic electronic parameters, such as the density of the localized states near the Fermi level, localization length, the hopping length, and the activation energy have been obtained. The change of the activation energy observed at high-temperature range was attributed to local structure distortions around Fe and Co atoms. The complicated behavior of charge transfer mechanisms is discussed based on two approaches: atomic disorder and electron correlations.

1. Introduction

The great interest in the borates as functional materials is due to their unique optical, luminescent, non-linear (NLO) and laser properties [1,2]. These compounds could have a wide application in spectroscopy and as a self doubling laser media [3,4]. The transition metal borates are attracting a special interest as magnetic semiconductors with strong electron correlations in 3*d* shell [5–7].

A family of heterometallic warwickites $Mg_{1-x}Co_xFeBO_4$ was recently characterized from the structural and magnetic points of view [8–10]. In particular, the compounds were identified by means of an X-ray crystallographic study, as belonging to the orthorhombic symmetry with space group *Pnma* [8]. Three kinds of ions Mg^{2+}, Co^{2+}, and Fe^{3+} are located at two structurally distinct octahedral sites 1 and 2. Four octahedra that share their edges are stacked in the sequence 2-1-1-2 (*row*). These rows are linked forming flat *ribbons* extending along the short *c*-axis.

In a X-ray diffraction structural refinement and Mössbauer study it has been shown that there is intrinsic disorder due to occupation of the octahedral sites by different metal atoms [8,9]. X-ray absorption spectroscopy (XAS) investigations reveal local structure distortions around the Fe and Co atoms gradually increasing with increasing Co content. Magnetic properties of $MgFeBO_4$, $Mg_{0.5}Co_{0.5}FeBO_4$, $CoFeBO_4$warwickites have been experimentally and theoretically studied [10]. It has been found that all these systems undergo a spin-glass transition at rather low temperatures ($T_{SG} = 10$, 20, and 22 K, respectively), where short range ordering sets-on. The mechanisms that give rise to the spin-glass behavior are: site occupation disorder by Fe^{2+}, Fe^{3+}, Co^{2+} at the 1 and 2 positions, and a high level of magnetic frustration caused by competing exchange interactions in triangular sublattices. The introduction of Co^{2+} induces uniaxial anisotropy with *b*-axis as the easy magnetization direction. In this paper, we describe the electronic transport properties of Mg-Co-Fe warwickite system obtained through electrical resistivity measurements.

The hetero metallic warwickites, $M^{2+}M'^{3+}BO_4$, where M^{2+}, M'^{3+} are transition metal ions, are expected to be insulating systems due to the combination of disorder effects and strong electronic correlations in the 3*d* shell of the transition metal cations. Instead, iron homo metallic warwickite ($M = M' = Fe$) is known to be semiconductor with rather small activation energies [11,12].

* Corresponding author at: Laboratory of Physics of Magnetic Phenomena, Kirensky Institute of Physics, Siberian Branch of Russian Academy of Science (IP SB RAS), Academgorodok 50/38, Krasnoyarsk 660036, Russia. Tel.: +7 (391)249 45 56.

E-mail address: nat@iph.krasn.ru (N.V. Kazak).

http://dx.doi.org/10.1016/j.jallcom.2015.04.056
0925-8388/

The Fe_2BO_4 was found to be a *L*-type ferrimagnet with a transition temperature of $T_N = 155$ K and the magnetic moments at the 1 sites being aligned antiparallel to those at the 2 sites, as deduced from neutron diffraction experiments. Mn_2BO_4 is anantiferromagnet with drastically smaller critical temperature of $T_N = 26$ K in comparison to Fe_2BO_4 [13–15]. Both materials display charge ordering (CO). At present, the nature of CO in the warwickites is a subject of intense discussion. The temperature dependence of CO in Fe_2BO_4 was extensively investigated by resistivity and differential scanning calorimetry measurements, Mössbauer spectroscopy, resonant X-ray diffraction, transmission electron microscopy, and electronic-structure calculations [16–22]. It was found that there is a commensurately charge ordered (CCO) phase below the CO transition temperature $T_{CCO} = 280$ K, with integer iron valence difference Fe^{2+} and Fe^{3+} alternating in the *a*-axis direction. The intermediate temperature range ($T_{CCO} < T < T_{CO}$, where $T_{CO} = 340$ K) is characterized by the onset of the temperature-dependent lattice incommensurate CO phase with presence of mobile and immobile carriers. Moreover, there is a valence fluctuating state (Fe^{2+}–Fe^{3+} electron hopping) above T_{CO}, i.e. above the structural transition from monoclinic to orthorhombic symmetry.

Fe_2BO_4 shows a broad semiconductor-to-semiconductor transition at ~317 K with a small decrease of the activation energy from 0.35 to 0.31 eV K [11]. Below the T_{CO} transition, the resistivity exhibits a broad anomaly and large thermal hysteresis. Pressure dependence of T_{CCO} and resistive switching in the incommensurate phase were characterized in a recent work [16]. Additionally, Leonov et al. [23] have presented a theoretical investigation of the electronic structure of the Fe_2BO_4 using the local spin density approximation (LSDA) + *U* method. They concluded that one needs to take into account a strong Coulomb interaction ($U = 5.5$ eV) for Fe to predict an insulating charge-ordered solution with the energy gap of 0.39 eV. *Ab initio* calculations and electron energy-loss spectroscopy (EELS) measurements have been performed on the CO state [22]. Electronic structure calculations using GGA + *U* predict a CO structure with a supercell of $2a \times b \times c$ and the CO modulation along the *a*-axis. Both local structural distortions and electrostatic repulsion were found to be important for the correct description of the CO state properties. An insulating state with an energy gap of 0.39 eV has been obtained for an *onsite* Coulomb repulsion $U = 4$ eV.

In spite of the success in the investigations of the homometallic iron warwickite there is a lack of electronic properties characterization of other members of the mentioned family. To the best of our knowledge, no electronic transport properties on heterometallic warwickites have been reported so far, except for $MgTiBO_4$ [24]. Marcucci et al. have performed a multiorbital tight-binding calculation of the electron structure and have shown that the Fermi level is located inside a Ti-3*d* band. The incorporation of the electronic correlations at the transition metal sites leads to a correlation gap near the Fermi level.

Thus, the electronic properties of the 3*d* warwickites need further studies, for example, on the effect of intrinsic disorder in site occupations as well as electron correlations on electrical transport.

In this respect, the purpose of the present study has been to investigate the conductivity mechanisms of the single crystal warwickites $MgFeBO_4$, $Mg_{0.5}Co_{0.5}FeBO_4$, and $CoFeBO_4$. The electrical conductivity measurements in the temperature range ($T = 210$–400 K) have allowed to identify a crossover from Mott's variable range hopping (VRH) to thermo-activation mechanism at a temperature T_{cr}. The influence of Co substitution on the resistivity has also been studied. The results are interpreted on the basis of the two key points, namely disorder and strong electron correlations.

2. Experimental details

Needle-shaped black crystals of $Mg_{1-x}Co_xFeBO_4$ warwickites were prepared using the flux method described in work [8] and their size was typically $0.5 \times 0.2 \times 5.0$ mm^3. Due to the high room temperature resistance of the sample (10^8 Ohm), the resistance was measured by a two-probe method using a teraohmmeter E6-13A with an accuracy better than 10%. The temperature interval has been from 400 K down to 210 K. The electrical contacts were made by soldering thin copper wires with indium-based paste. The resistivity was measured along the needle, which corresponds to the *c*-axis direction.

3. Experimental results and discussion

3.1. Identification of the conductivity mechanisms

The temperature dependence of the resistivity $\rho(T)$ is very similar for $MgFeBO_4$, $Mg_{0.5}Co_{0.5}FeBO_4$ and $CoFeBO_4$, showing a monotonic decrease with *T* (Fig. 1). We note that the resistivity for all studied samples varied by ~ four orders of magnitude with temperature reduction from 400 to 200 K. Such a large variation interval is important for accurate analysis of hopping conduction.

All curves at the high-temperature phase show clear straight-line behavior in a $\log\rho_a$ versus $1/T$ plot (Fig. 2). However, strong deviations from linearity arise as temperature is decreased. The distribution of the metal atoms over non-equivalent sites creates disorder and the low-temperature electronic properties of the warwickites can be considered as akin to those of disordered semiconductors, where electron localization and hopping conduction play a significant role. As a consequence, different conductivity mechanisms can prevail in different temperature intervals.

The general expression for the hopping conductivity is

$$\rho(T) = \rho_0(T)\exp\left[(T_0/T)^p\right], \quad (1)$$

where the pre-factor depends on temperature as $\rho_0(T) = AT^m$, T_0 is the characteristic temperature and *A* is a constant. The exponents *p* and *m* depend on the hopping charge transfer mechanism and are interrelated. The values of $p = 1$, 1/4 or 1/2 describe the 3D nearest-neighbor hopping (NNH), the variable-range hopping (VRH) of Mott type [25] or Efros–Shklovskii (ES) type [26], respectively. For materials in which the density of states at the Fermi level ε_F is suppressed by Coulomb electron–electron interactions, VRH is expected to follow the ES model. Otherwise, if such correlations are unimportant the conductivity obeys the Mott VRH law. The nearest-neighbor hopping (NNH) conductivity is given by $m = p = 1$. In the ES regime the prefactor in Eq. (1) $\rho_0 \sim T^{1/2}$ or $\sim T^{-3/2}$ for the presence or absence of a fluctuating short-range potential [26]. In the Mott regime the value of the exponent

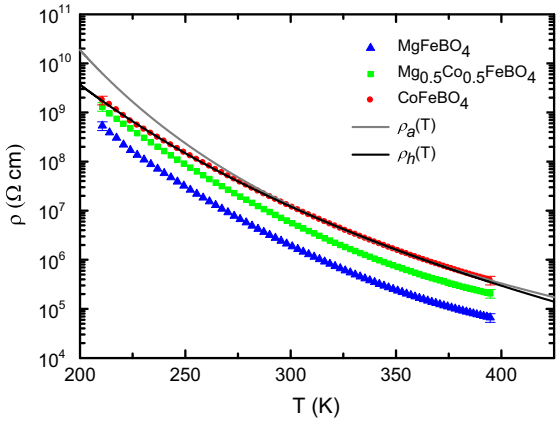

Fig. 1. The temperature dependencies of resistivity. The $\rho_a(T)$ and $\rho_h(T)$ are the high-and low-temperature contributions to the conductivity, respectively, calculated using the fits parameters (see Table 1).

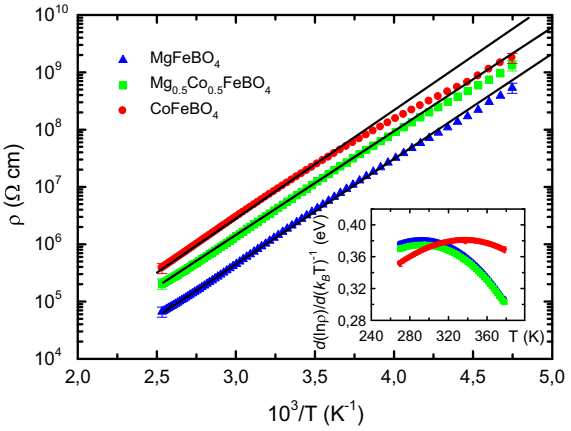

Fig. 2. The activated behavior of the resistivity at high temperatures. The inset shows the temperature dependence of the activation energy.

$m = 1/4, -3/4$ have been proposed depending of the details of the applied model [26].

We have estimated the exponents p and m in a self-consistent way using the reduced activation energy:

$$w = -\frac{d\ln\rho(T)}{d\ln T} = -m + p\left(\frac{T_0}{T}\right)^p. \quad (2)$$

Fig. 3 shows the logarithmic derivative w versus logarithmic T plot for $MgFeBO_4$ as an example. It is clearly seen that the $\ln w$ curve demonstrates the monotonic drop with temperature. The slope of the plot is not constant, indicating a change of conduction mechanism. The curve data can be divided into two temperature ranges with different slopes, i.e. ~210–270 K (LT) and 280–400 K (HT). A least square fit of the LT data gives the following estimation: $p = 0.23 \pm 0.01$, 0.24 ± 0.02, 0.21 ± 0.02 for $x = 0.0$, 0.5, and 1.0, respectively, at $m = 0$. The obtained values are close to 0.25, as expected for 3D Mott VRH. In Fig. 3, for clarity, two temperature intervals corresponding $p \approx 0.23$ and 1.01 are shown.

A similar analysis was applied to the high-temperature (HT) $\rho(T)$ data, and the p values obtained are: $p = 1.01 \pm 0.03$, 0.99 ± 0.03, 0.97 ± 0.02 for $x = 0.0$, 0.5, and 1.0, respectively. To explain the high-temperature experimental data we have considered two models of conduction: the simple thermo-activation and NNH. The theoretical curves were calculated and both models fit the data well. Nevertheless, the straight line fitted to these curves yields a better linear correlation coefficient for thermo-activation conductivity than that for NNH, *e.g.* $R = 0.99943$ for nearest neighbor hopping ($m = p = 1$) and $R = 0.99991$ for thermo-activation conductivity ($m = 0$, $p = 1$) for $MgFeBO_4$ as an example. So, we conclude that electrical conductivity of the Mg-Co-Fe warwickites is determined by the superposition of two mechanisms: the LT Mott VRH $\rho_h(T)$ and HT thermo-activated $\rho_a(T)$ (Fig. 2).

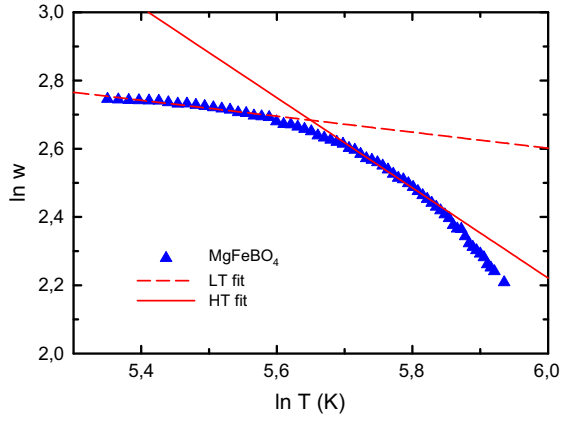

Fig. 3. Reduced activation energy w plotted versus temperature T in a log–log scale. The straight lines are the fits to the low- and high- temperature intervals with $p = 0.23 \pm 0.01$ and 1.01 ± 0.03, respectively. Results for $MgFeBO_4$.

3.2. VRH conductivity

A consistent approach to analyze the VRH conductivity needs to take into account the temperature dependence of the prefactor $\rho_0(T)$. The Mott type of hopping conductivity is determined fitting a linear dependence to the data represented in terms of $\ln(\rho_h/T^m)$ versus T^{-p}. We put $m = p = 1/4$, a case of hydrogenic wavefunctions of the localized electrons realizing in the doped crystalline semiconductors with shallow impurities at low temperatures [26]. The best fits are shown in Fig. 4, and the fit parameters for A in the VRH model, A_{VRH}, and T_0 are given in Table 1. A straight lines fitted to these curves yield R coefficients = 0.99935, 0.99938 and 0.99985 for $x = 0.0$, 0.5, 1.0 respectively. The characteristic temperature T_0 for the Mott conductivity is given by the known expression:

$$T_0 = \frac{B}{k_B N(\varepsilon_F)\xi^3} \quad (3)$$

Here $N(\varepsilon_F)$ is the density of states (DOS) at the Fermi energy, ξ is the localization length and $B = 21$ is a constant [26].

The VRH conductivity is very sensitive to the wave function type of the localized carriers, on the spatial decay of the wave function given by the localization length ξ, and on the one-electron DOS near the Fermi level $N(\varepsilon_F)$. The two latter parameters are important for the electronic structure analysis and require an independent determination. We used the following assumptions. The wave function of the carriers is concentrated near the localization centers, notably the metal atoms, and decays with distance as $\varphi \sim \exp\left(-\frac{r}{\xi}\right)$. Due to the overlapping of the exponential tails there is a finite probability for hopping. The $T^{-\frac{1}{4}}$ law takes effect when hopping length R_h exceeds the localization radius ($R_h > \xi$) and is given by

$$R_h = \frac{3}{8}\xi\left(\frac{T_0}{T}\right)^{\frac{1}{4}} \quad (4)$$

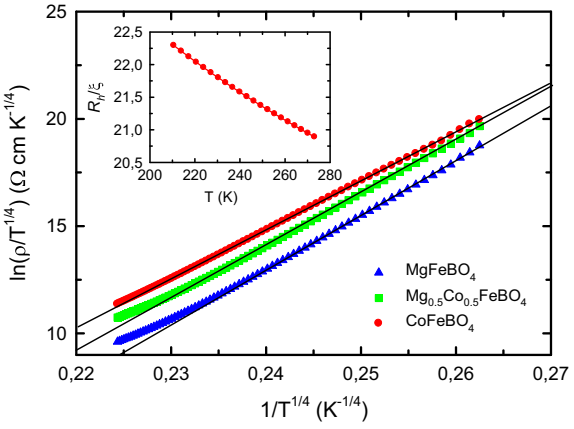

Fig. 4. The temperature dependence of the modified resistivity $\rho/T^{1/4}$ in the VRH range. The straight lines are the linear fits. The upper inset is the ratio of the hopping length R_h to the localization length ξ as the function of the temperature plotted for $CoFeBO_4$.

Table 1
The fits parameters for the hopping and the activation conductivities obtained in various temperature intervals. The values of exponents $p = m = 1/4$ for Mott VRH regime. The parameter T^* means the temperature corresponding to the maximum of the activation energy E_a^*.

	Mott VRH		Activation conductivity			
	A_{VRH} (Ω cm $K^{-1/4}$)	$T_0 \cdot 10^9$ (K)	A_{act} (Ω cm)	E_a (eV)	T^* (K)	E_a^* (eV)
$MgFeBO_4$	$(1.05 \pm 0.36) \cdot 10^{-21}$	4.26 ± 0.09	1.23 ± 0.05	0.368 ± 0.002	292	0.379 ± 0.002
$Mg_{0.5}Co_{0.5}FeBO_4$	$(2.78 \pm 0.47) \cdot 10^{-20}$	3.68 ± 0.04	4.42 ± 0.14	0.364 ± 0.002	295	0.375 ± 0.002
$CoFeBO_4$	$(7.35 \pm 2.28) \cdot 10^{-18}$	2.63 ± 0.06	7.37 ± 0.23	0.369 ± 0.002	337	0.379 ± 0.002

Putting $\xi = r_0 \approx N_0^{-1/3} \approx 3.24$ Å, where N_0 is the metal atom concentration, we obtain with Eqs. (3) and (4) the values of R_h and $N(\varepsilon_F)$ (Table 2). The values of $N(\varepsilon_F)$ obtained for the three warwickites are of the order of 10^{18} and typical for usual oxide semiconductors [27]. The hopping energy ε can be defined as the energy required for the carrier transfer between two localized states centered at different locations. The charge carriers are moved with a minimal change in the energy ε. Upon cooling, the energy interval around Fermi level $\Delta\varepsilon = \varepsilon_F \pm \varepsilon$, which corresponds to the localized states participating in hopping conductivity, is narrowed and the average hopping length R_h increases (inset Fig. 4). The monotonic dependence of R_h versus T indicates that the charge state of the localization centers is invariable and the potential relief is a monotonically changing function. In the presence of an electrical field the charge carriers move within a hopping range R_h almost 20 times exceeding the localization radius ξ.

The activation energy determining the sample's hopping conductivity at a given temperature is given by the expression [25]

$$\varepsilon = \frac{3}{4\pi R_h^3 N(\varepsilon_F)} \tag{5}$$

The Mott parameters, such as DOS $N(\varepsilon_F)$, hopping energy ε, hopping length R_h, and localization length ξ, have been estimated using Eqs. (3)–(5) at 260 and 210 K (Table 2). It is observed that the hopping energy ε is of the order of a few k_BT and decreases with temperature reduction. As can be seen from Eq. (1), within the VRH range, ε should depend on the temperature as $T^{3/4}$. Fig. 5 shows the linearization of ε in coordinates of $\frac{d(\ln \rho(T))}{d(k_BT)^{-1}}$ versus $T^{3/4}$. The best linearization is obtained for the LT interval as expected. The hopping energies ε calculated with Eq. (5) (see Table 2) are in a good agreement with the experimental value presented in Fig. 5.

3.3. Thermo-activated conductivity

As the temperature increases, the energy scale is changed and the thermo-activation conductivity mechanism becomes prevalent. The fitting parameters for the HT interval are collected in Table 1. It is seen that the activation energy $E_a \approx 0.37$ eV is similar for all samples. The local activation energy $E_a = \frac{d(\ln \rho_a)}{d(k_BT)^{-1}}$ obtained by the direct differentiation of the experimental data $\rho(T)$ as a function of the temperature is depicted in Fig. 2 inset. In general, the behavior is similar for all samples, showing a monotonic rise at low temperatures and a slowing down at T^*. The highest values of the activation energy E_a^* were found to be close to 0.38 eV (Table 1). The activation energy decreases with further heating.

Table 2
Mott parameters of the Mg–Co–Fe warwickites for the LT regime.

	T (K)	$N(\varepsilon_F) \cdot 10^{18}$ (eV^{-1} cm^{-3})	ε (eV)	$\xi \cdot 10^{-8}$ (cm)	$R_h \cdot 10^{-8}$ (cm)	R_h/ξ
	260					
$MgFeBO_4$		1.68	0.307	3.24	77.3	23.8
$Mg_{0.5}Co_{0.5}FeBO_4$		1.96	0.296	3.23	74.3	23.0
$CoFeBO_4$		2.75	0.272	3.23	68.3	21.1
	210					
$MgFeBO_4$		1.68	0.262	3.24	81.5	25.2
$Mg_{0.5}Co_{0.5}FeBO_4$		1.96	0.252	3.23	78.4	24.2
$CoFeBO_4$		2.75	0.232	3.23	72.1	22.3

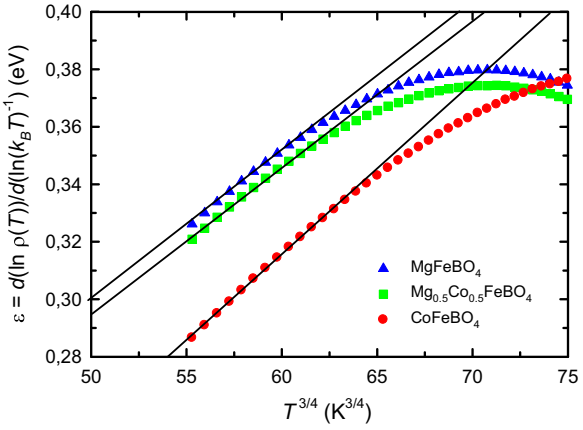

Fig. 5. The VRH's activation energy ε versus $T^{3/4}$. The straight lines are the linear fittings.

3.4. Discussion

Numerous theoretical investigations on the oxyborates band structure have been made using the LSDA, GGA ($U = 0$), LSDA + U, GGA + U and *ab initio* calculation of molecular orbitals [22,23,28–30]. Single electron calculations data yield electronic states near the ε_F mainly constituted by the 3d orbitals of the TM, which results in a metallic ground state. This conclusion is in contrast with the experimental data on the TM oxyborates, such as Fe_2BO_4, $Fe_{1.91}V_{0.09}BO_4$, $FeBO_3$, VBO_3, which have an insulating state at low temperatures. However, the assumption of strong Coulomb interaction ($U < 6$ eV) results in an insulating state solution with the energy gap opening at the ε_F.

To understand the electronic transport properties of Mg-Co-Fe warwickites, the coexistence of magnetic disorder and correlation effects should be taken into account. The disorder effect manifests itself in the VRH transport behavior at low temperatures. The intrinsic atomic disorder present in the studied samples leads to the appearance of a random perturbing potential. The Fermi level occurs in the region of localized states, that results in the appearance of a pseudogap with mobility edges, ε_{c1} at the conduction band bottom and ε_{c2} at the valence band top. At high temperatures the conductivity is determined by the carriers excited to the mobility edges and $\rho(T) \sim \exp(E_a/T)$, where $E_a = \varepsilon_c - \varepsilon_F$. The activation energy E_a obtained from the fitting of HT data is ~0.37 eV and defines the value of the mobility edge ε_c for all studied warwickites. This value is in good agreement with the early reported experimental data ($E_a = 0.35$ eV) and theoretical calculations on Fe_2BO_4 ($\varepsilon_g = 0.39$ eV) [22,23]. As the temperature decreases the deviation from the linearity in ln ρ versus $1/T$ occurs and the disorder energy plays a dominant role. The conductivity is determined by the

carriers hopping over localized states near the Fermi level ε_F. The Mott's conductivity type assumes that at energies ε far from ε_F ($|\varepsilon - \varepsilon_F| \gg \varepsilon_F$) the DOS $N(\varepsilon) \approx N(\varepsilon_F)$ = constant and the carriers may have enough energy to overcome the Coulomb gap Δ_{CG} at all measured temperatures ($k_BT > \Delta_{CG}$. Using the data at the lowest reached temperature we have estimated the $\Delta_{CG} < 0.017$ eV for all samples. The absence of the ES correlated hopping conductivity reveals that the electron correlations which are responsible for the insulator ground state of the ideal perfect crystal are not present in our case. The defect originated charge carriers in the studied samples have weakly correlated electronic states in the narrow vicinity of the Fermi level.

The characteristic temperature T_0 was found to be of the order of 10^9 K indicating high localization energy of the charge carriers. This value of T_0 is of the order of magnitude of some manganites ($Pr_{0.7}Pb_{0.3}MnO_3$) $T_0 \approx 10^9$ [27], and rather large in comparison to those obtained for oxide semiconductors and thin films which vary from 10^6 to 10^7 K [31–33]. The Co substitution leads to a slight reduction of T_0 and an increase in $N(\varepsilon_F)$ and can testify the weakening of the localization. The latter implies the decrease of the hopping energy ε required for the carrier transfer (0.33 and 0.28 eV for x = 0.0 and 1.0, respectively) and the shortening of R_h, the average distance between two localized states participating in hopping conductivity. Thus, Co substitution makes the charge transfer between two localized states easier. With temperature decrease the hops with large R_h become energetically favorable.

So, we conclude that the resistivity of $Mg_{1-x}Co_xFeBO_4$ at a given temperature is the superposition of two contributions $\rho(T) = \rho_h(T) + \rho_a(T)$. The first term corresponds to variable range hopping of non-interacting carriers and the second has the thermo-activation character. The crossover temperature between both channels was found to be the same for all samples $T_{cr} \sim 280$ K. The fact that the macroscopic parameters do not depend on the Co-concentration indicates that for all studied samples the electronic structure near the Fermi level is common. The observed broad electronic transition at 290–340 K can result either from a monotonic reduction of one of the conductivity contributions, or an activation energy with temperature dependence. The latter assumption is reasonable in view of the local structure study results [8]. The recent XAS experiments have revealed temperature- and substitution- induced local distortions of the coordination octahedra around both Fe and Co atoms. These distortions are accompanied by bond lengths compression along one of the octahedron nominal 4-fold axis and elongation in the perpendicular plane being more pronounced for $CoFeBO_4$. Since distorted bonds mean a disordered lattice and hence a variation in the energy barrier for the carriers transfer, one may expect these distortions to explain activation energy temperature dependence.

4. Conclusions

We have investigated the influence of the temperature and Co-addition on the electronic transport properties of $Mg_{1-x}Co_xFeBO_4$ with x = 0.0, 0.5, and 1.0, paying major attention to the resistivity behavior and the conductivity mechanisms in a broad temperature interval. The Mott variable-range hopping and thermo-activation conductivity mechanisms have been identified in various temperature intervals. The microscopic parameters, such as the density of the localized states near the Fermi level $N(\varepsilon_F)$, the hopping length R_h, localization length ξ, hopping energy ε, and the activation energy E_a have been determined. The Co dependence of the parameters has been discussed. The value of Coulomb gap Δ_{CG} has been estimated. The qualitative analysis of electron structure based on two main ingredients – atomic disorder and electron correlations has been made. As a result of this, the studied warwickites have been classified as disordered correlated systems.

Acknowledgments

This work has been financed by Council for Grants of the President of the Russian Federation (Project Nos. NSh-2886.2014.2, SP-938.2015.5), Russian Foundation for Basic Research (Project Nos. 13-02-00958-a, 13-02-00358-a, 14-02-31051-mol-a). The work of one of coauthors (M.S.P.) was supported by the grant of KSAI "Krasnoyarsk Regional Fund of Supporting Scientific and Technological Activities" and by the Program of Foundation for Promoting the Development of Small Enterprises in Scientific and Technical Sphere ("UMNIK" program). Financial support from the Spanish MINECO MAT11/23791 and DGA IMANA project E-34 is acknowledged.

References

[1] C. Chen, Y. Wang, B. Wu, K. Wu, W. Zeng, L. Yu, Nature 373 (1995) 322–324.
[2] H. Nakao, M. Nishida, T. Shikida, H. Shimizu, H. Takeda, T. Shiosaki, J. Alloys Comp. 408–412 (2006) 582–585.
[3] D. Jaque, O. Enguita, J. Garcia Sole, A.D. Jiang, Z.D. Luo, Appl. Phys. Lett. 76 (2000) 2176.
[4] M. Huang, Y. Chen, X. Chen, Y. Huang, Z. Luo, Opt. Commun. 208 (2002) 163–166.
[5] I. Mitov, Z. Cherkezova-Zheleva, V. Mitrov, B. Kunev, J. Alloys Comp. 289 (1999) 55–65.
[6] H. Yamane, T. Kawano, K. Fukuda, T. Suehiro, T. Sato, J. Alloys Comp. 512 (2012) 223–229.
[7] D. Afanasiev, I. Razdolski, K.M. Skibinsky, D. Bolotin, S.V. Yagupov, M.B. Strugatsky, A. Kirilyuk, Th. Rasing, A.V. Kimel, Phys. Rev. Lett. 112 (2014). 147403(1-5).
[8] N.V. Kazak, M.S. Platunov, Yu.V. Knyazev, N.B. Ivanova, Y.V. Zubavichus, A.A. Veligzhanin, A.D. Vasiliev, L.N. Bezmaternykh, O.A. Bayukov, A. Arauzo, J. Bartolomé, K.V. Lamonova, S.G. Ovchinnikov, (submitted to Phys. Status Solidi B).
[9] I.S. Lyubutin, N.Yu. Korotkov, K.V. Frolov, N.V. Kazak, M.S. Platunov, Yu.V. Knyazev, L.N. Bezmaternyh, S.G. Ovchinnikov, A. Arauzo, J. Bartolomé, J. Alloys and Comp. (2015), http://dx.doi.org/10.1016/j.jallcom.2015.04.067.
[10] A. Arauzo, N.V. Kazak, N.B. Ivanova, M.S. Platunov, Yu.V. Knyazev, O.A. Bayukov, L.N. Bezmaternykh, I.S. Lyubutin, K.V. Frolov, S.G. Ovchinnikov, J. Bartolomé, J. Magn. Magn. Mater. (2015), submitted for publication, ArXiv: 1504.05912.
[11] J.P. Attfield, A.M.T. Bell, L.M. Rodriguez-Martinez, J.M. Greneche, R.J. Cernik, J.F. Clarke, D.A. Perkins, Nature 396 (1998) 655–658.
[12] J.P. Attfield, A.M.T. Bell, L.M. Rodriguez-Martinez, J.M. Greneche, R. Retoux, M. Leblanc, R.J. Cernik, J.F. Clarkeand, D.A. Perkins, J. Mater. Chem. 9 (1999) 205–209.
[13] R. Norrestam, M. Kritikos, A. Sjdin, J. Solid State Chem. 114 (1995) 311–316.
[14] R.J. Goff, A.J. Williams, J.P. Attfield, Phys. Rev. B 70 (2004) 014426.
[15] N.V. Kazak, M.S. Platunov, Yu.V. Knyazev, N.B. Ivanova, O.A. Bayukov, A.D. Vasiliev, L.N. Bezmaternykh, V.I. Nizhankovskii, S.Yu. Gavrilkin, K.V. Lamonova, S.G. Ovchinnikov, J. Magn. Magn. Mater. (2015), submitted for publication, ArXiv: 1504.05870.
[16] A. Akrap, M. Angst, P. Khalifah, D. Mandrus, B.C. Sales, L. Forró, Phys. Rev. B 82 (2010). 165106(1-7).
[17] G.R. Hearne, W.N. Sibanda, E. Carleschi, V. Pischedda, J.P. Attfield, Phys. Rev. B 86 (2012) 195.
[18] M. Angst, P. Khalifah, R.P. Hermann, H.J. Xiang, M.-H. Whangbo, V. Varadarajan, J.W. Brill, B.C. Sales, D. Mandrus, Phys. Rev. Lett. 99 (2007). 086403(1-4).
[19] H.X. Yang, H.F. Tian, Y.J. Song, Y.B. Qin, Y.G. Zhao, C. Ma, J.Q. Li, Phys. Rev. Lett. 106 (2011). 016406(1-4).
[20] M. Angst, R.P. Hermann, W. Schweika, J-W. Kim, P. Khalifah, H.J. Xiang, M.-H. Whangbo, D.-H. Kim, B.C. Sales, D. Mandrus, Phys. Rev. Lett. 99 (2007). 256402(1-4).
[21] S.R. Bland, M. Angst, S. Adiga, V. Scagnoli, R.D. Johnson, J. Herrero-Martín, P.D. Hatton, Phys. Rev. B 82 (2010). 115110(1-10).
[22] Z. Chen, C. Ma, Y.J. Song, H.X. Yang, H.F. Tian, J.Q. Li, Phys. Rev. B 86 (2012). 045111(1-6).
[23] I. Leonov, A.N. Yaresko, V.N. Antonov, J.P. Attfield, V.I. Anisimov, Phys. Rev. B 72 (2005). 014407(1-7).
[24] D.C. Marcucci, A. Latgé, E.V. Anda, M. Matos, J.C. Fernandes, Phys. Rev. B 56 (1997) 3672–3677.
[25] N.F. Mott, Metal-insulator transitions, Taylor and Francis, London, 1974.

[26] B.I. Shklovskii, A.L. Efros, Electronic Properties of Doped Semiconductors, Springer-Verlag, Berlin, 1984.
[27] M. Viret, L. Ranno, J.M.D. Coey, Phys. Rev. B 55 (1997) 8067–8070.
[28] A.V. Postnikov, St. Bartkowski, M. Neumann, R.A. Rupp, E.Z. Kurmaev, S.N. Shamin, V.V. Fedorenko, Phys. Rev. B 50 (1994) 14849–14853.
[29] K. Parlinski, Eur. Phys. J. B 27 (2002) 283–285.
[30] N.B. Ivanova, V.V. Rudenko, A.D. Balaev, N.V. Kazak, V.V. Markov, S.G. Ovchinnikov, I.S. Edelman, A.S. Fedorov, P.V. Avramov, JETP 94 (2002) 299–306.
[31] J.C. Gonzalez, G.M. Ribeiro, E.R. Viana, P.A. Fernandes, P.M.P. Salome, K. Gutierrez, A. Abelenda, F.M. Matinaga, J.P. Leitao, A.F. da Cunha, J. Phys. D: Appl. Phys. 46 (2013). 155107(1-7).
[32] A.K. Singh, A. Dhillon, T.D. Senguttuvan, A.M. Siddiqui, Int. J. Curr. Eng. Technol. 4 (2014) 399–404.
[33] A.A. Kozlovskii, V.F. Khirnyi, A.V. Semenov, V.M. Puzikov, Phys. Solid State 53 (2011) 707–716.